

**This item is the archived peer-reviewed author-version of:**

Progressive motor deficit is mediated by the denervation of neuromuscular junctions and axonal degeneration in transgenic mice expressing mutant (P301S) Tau protein

**Reference:**

Yin Zhuoran, Valkenburg Femke, Hornix Betty, Mantingh-Otter Ietje, Zhou Xingdong, Mari Muriel, Reggiori Fulvio, Van Dam Debby, Eggen Bart J.L., De Deyn Peter Paul, ....- Progressive motor deficit is mediated by the denervation of neuromuscular junctions and axonal degeneration in transgenic mice expressing mutant (P301S) Tau protein  
Journal of Alzheimer's disease - ISSN 1387-2877 - (2017), p. 1-17  
Full text (Publishers DOI): <http://dx.doi.org/doi:10.3233/JAD-161206>

# Progressive Motor Deficit is Mediated by the Denervation of Neuromuscular Junctions and Axonal Degeneration in Transgenic Mice Expressing Mutant (P301S) Tau Protein

Zhuoran Yin<sup>a,b,1</sup>, Femke Valkenburg<sup>c,1</sup>, Betty E. Hornix<sup>d</sup>, Ietje Mantingh-Otter<sup>a</sup>, Xingdong Zhou<sup>e,f</sup>, Muriel Mari<sup>e</sup>, Fulvio Reggiori<sup>e</sup>, Debby Van Dam<sup>c,g</sup>, Bart J.L. Eggen<sup>a</sup>, Peter P. De Deyn<sup>c,g,h</sup> and Erik Boddeke<sup>a,\*</sup>

<sup>a</sup>*Department of Neuroscience, Section Medical Physiology, University Medical Center Groningen, University of Groningen, Groningen, The Netherlands*

<sup>b</sup>*Department of Medical Ultrasound, Tongji Hospital, Tongji Medical College, Huazhong University of Science and Technology, Wuhan, China*

<sup>c</sup>*Laboratory of Neurochemistry and Behavior, Institute Born-Bunge, University of Antwerp, Antwerp, Belgium*

<sup>d</sup>*Department of Neurobiology, Groningen Institute for Evolutionary Life Science, University of Groningen, Groningen, The Netherlands*

<sup>e</sup>*Department of Cell Biology, University Medical Center Groningen, University of Groningen, Groningen, The Netherlands*

<sup>f</sup>*Department of Preventive Veterinary Medicine, College of Veterinary Medicine, Northeast Agricultural University, Harbin, China*

<sup>g</sup>*Department of Neurology and Alzheimer Research Center, University Medical Center Groningen, University of Groningen, Groningen, The Netherlands*

<sup>h</sup>*Biobank, Institute Born-Bunge, Antwerp, Belgium*

Accepted 23 January 2017

**Abstract.** Tauopathies include a variety of neurodegenerative diseases associated with the pathological aggregation of hyperphosphorylated tau, resulting in progressive cognitive decline and motor impairment. The underlying mechanism for motor deficits related to tauopathy is not yet fully understood. Here, we use a novel transgenic tau mouse line, Tau 58/4, with enhanced neuron-specific expression of P301S mutant tau to investigate the motor abnormalities in association with the peripheral nervous system. Using stationary beam, gait, and rotarod tests, motor deficits were found in Tau 58/4 mice already 3 months after birth, which deteriorated during aging. Hyperphosphorylated tau was detected in the cell bodies and axons of motor neurons. At the age of 9 and 12 months, significant denervation of the neuromuscular junction in the extensor digitorum longus muscle was observed in Tau 58/4 mice, compared to wild-type mice. Muscle hypotrophy was observed in Tau 58/4 mice at 9 and 12 months. Using electron microscopy, we observed ultrastructural changes in the sciatic nerve of 12-month-old Tau 58/4 mice indicative of the loss of large axonal fibers and hypomyelination (assessed by g-ratio). We conclude that the accumulated hyperphosphorylated tau in the axon terminals may induce dying-back axonal degeneration,

<sup>1</sup>These authors contributed equally to this work.

\*Correspondence to: Erik Boddeke, Department of Neuroscience, Section Medical Physiology, University Medical Center

Groningen, Antonius Deusinglaan 1, Groningen, 9713 AV, The Netherlands. Tel.: +31 503616443; Fax: +31 503632751; E-mail: h.w.g.m.boddeke@umcg.nl.

myelin abnormalities, neuromuscular junction denervation, and muscular atrophy, which may be the mechanisms responsible for the deterioration of the motor function in Tau 58/4 mice. Tau 58/4 mice represent an interesting neuromuscular degeneration model, and the pathological mechanisms might be responsible for motor signs observed in some human tauopathies.

Keywords: Alzheimer's disease, axonal degeneration, motor dysfunction, neuromuscular junction denervation, tauopathy

## INTRODUCTION

Tauopathies comprise various neurodegenerative diseases characterized by the pathological accumulation of hyperphosphorylated microtubule-associated protein tau (MAPT) in the nervous system. Most tauopathies, including Alzheimer's disease (AD), frontotemporal dementia with parkinsonism linked to chromosome 17 (FTDP-17), progressive supranuclear palsy (PSP), and corticobasal degeneration (CBD) cause dementia or degeneration of the motor system [1]. In AD, motor signs have been described in long term follow-up of large AD cohorts. Some of the motor signs are due to mixed pathologies and/or the involvement of neuropathological lesions in substantia nigra, striatum, and mesocortical pathways, etc. [2, 3]. FTDP-17, PSP, and CBD share some motor deficits with Parkinson's disease including bradykinesia, tremors, and rigidity, which occur at an early stage of the disease [4]. Until now, no symptomatic treatment for FTDP-17, CBD, or PSP has been approved by the US Food and Drug Administration. Off-label use of symptomatic medication for motor symptoms such as levodopa is based on clinical experience [5], but the percentage of levodopa resistance in tauopathies remains high [5, 6]. Loss of dopaminoreceptive neurons in substantia nigra may be one of the reasons for the levodopa-resistant motor dysfunction in tauopathy [7]. Disturbance of axonal transport has also been indicated as a possible mechanism for motor deficits in transgenic tauopathy mouse models [8]. Clearly, further research on peripheral nerve pathology and motor function in tauopathies is required to better understand the underlying mechanisms and to provide new therapeutic possibilities for motor impairment in tauopathy.

Tau, as one of the major microtubule-associated proteins, is important for stabilization of microtubules and maintenance of axoplasmic flow [9]. Several mutations in the tau gene have been identified in FTDP-17 families, e.g., exon 10 (P301L, P301S, N279K), exon 9 (G257T, G272V), exon 12 (V337M), or exon 13 (R406W) [10], which all appear to alter the conformation of the protein. Consequently, mutant tau has a higher affinity for brain protein kinases, phosphorylates at a faster rate, self-aggregates more

easily into paired helical filaments and, subsequently, into neurofibrillary tangles [9]. Abnormal accumulation of hyperphosphorylated tau leads to pathological alterations in neuronal structures including dystrophic neurites observed in AD, which is characterized by the disorganization of the microtubule- and neurofilament network [11]. Hyperphosphorylated tau can disassemble microtubules, which may block axoplasmic flow and induce retrograde neuronal degeneration [9]. Restoration of microtubule stabilization has been demonstrated to improve axonal transport and motor symptoms in transgenic tau mice [12]. Axonal transport could, therefore, be a future therapeutic target for tauopathy [13].

Various transgenic mouse models for tau pathology have been generated [14], which show many features of human tauopathy. Expression of FTDP-17-related (e.g., P301L/S, V337M, and R406W) mutant tau proteins in transgenic mice, induces symptoms of human tauopathy, such as motor disturbances and memory loss [14–16]. Loss of functional synapses and axon degeneration were also observed in transgenic tau mouse models [8, 17, 18]. The phenotype of tau mouse models depends on the tau mutation, promoters, and tau isoform composition [15, 17, 19]. Understanding pathological alterations and phenotypic changes in tau transgenic mouse models may provide new insight into the onset and development of human tauopathy [17].

The current study focuses on a novel mouse model Tau 58/4, which contains the point mutation P301S in exon 10 of the human MAPT gene under regulation by the neuron-specific Thy-1.2 promoter. As a consequence, mutant tau proteins distribute both in neuronal somata and axonal compartments. A battery of motor tests, including gait analysis, the stationary beam test, the hindlimb clasping test, and rotarod performance were applied to evaluate the motor function of Tau 58/4 mice. By immunofluorescence staining, the percentage of partially innervated and denervated neuromuscular junctions was quantified in the extensor digitorum longus (EDL) muscle. Using electron microscopy, ultrastructural alterations of axons were observed in the sciatic nerve of 12-month-old Tau 58/4 mice. Our data suggest that the expression of human transgenic tau in the motor

neurons impairs axonal function and the maintenance of neuromuscular junctions. Subsequently, it leads to muscle denervation, which could be one of the underlying mechanisms of the deteriorating motor function observed during aging in Tau 58/4 mice.

## MATERIALS AND METHODS

### *Tau 58/4 transgenic mice*

Generation of transgenic mice was performed as described previously [20]. Briefly, to create the Tau58/4 construct, a F115 TAU cDNA encoding the human tau isoform (0N4R) containing the P301S mutation was cloned into the pTSC21K bacterial expression vector including the murine Thy1.2 gene [21] using the XhoI restriction site. Vector sequences were removed by NotI PvuI digestion. Injection and manipulation of mice was identical to described procedures [20]. Tau 58/4 mice were generated in a hybrid C57BL/6 × DBA2 background, and then the mice were backcrossed to C57BL/6J to create an isogenic line. The 58/4 transgenic line is fertile and produces normal sized litters. Only heterozygous, male mice were used for experiments.

Mice were weaned 4 weeks after birth and group housed with littermates of the same sex. Food and water were supplied *ad libitum*. Custom primers were used for genotyping by PCR analysis with ear punches, collected from mice aged approximately 4 weeks, as source of DNA. Motor tests and surgical procedures were performed during the light phase of the animals, and all mice were acclimatized for at least 1h before conducting the experiments. Experimenters were blinded to the genetic status of the animals. All experiments were carried out in

compliance with the European Community Council Directive (2010/63/EU) and were approved by the Animal Ethics Committee of the University of Antwerp (ECD 2013–31).

### *Behavioral tests*

Male heterozygous (HET) mice and wild-type (WT) control littermates aged 3, 6, 9, and 12 months were subjected to a battery of motor function-related behavioral tests. The numbers of used animals are listed in Table 1.

#### *Hindlimb clasping test*

Animals were suspended by the tail and kept at a height of 40 cm above the able top for a duration of 30 s, during which the presence of hindlimb clasping behavior was observed.

#### *Gait analysis*

Gait characteristics (stride length, toe span, and track width) were analyzed by applying ink to the hind paws of the animals. Mice were then allowed to walk on a strip of paper in a brightly lit walk lane (width: 4.5 cm, length: 40 cm), toward a dark goal box. At least 2 complete gait patterns from each mouse were obtained on which gait characteristics were measured by caliper.

#### *Stationary beam test*

The stationary beam test of equilibrium and balance was performed on a wooden beam (diameter: 25 mm, length: 110 cm) covered with a layer of masking tape to provide a firm grip. The beam was divided into 11 segments and placed at a height of 38 cm above a cushioned bench. The ends of the beam

Table 1

Motor function-related parameters obtained with the tests applied to assess the motor function of the Tau 58/4 mice in comparison with age-matched WT littermates

Tau 58/4	Age	3 months		6 months		9 months		12 months	
		WT (n=9)	HET (n=10)	WT (n=11)	HET (n=11)	WT (n=11)	HET (n=12)	WT (n=15)	HET (n=16)
<i>Stationary Beam test</i>									
	Number of segments	60 ± 9	20 ± 3**	48 ± 8	14 ± 6**	42 ± 10	10 ± 5*	25 ± 6	6 ± 2*
	Number of falls	0.2 ± 0.1	1.5 ± 0.5*	0.5 ± 0.3	0.9 ± 0.3	0	1.8 ± 0.4**	0.5 ± 0.2	2.3 ± 0.3***
	Latency to first fall (s)	232 ± 6	211 ± 10	217 ± 14	201 ± 11	233 ± 7	169 ± 19**	222 ± 7	141 ± 15***
<i>Gait Analysis</i>									
	Stride length left (mm)	63 ± 3	62 ± 2	62 ± 2	49 ± 2***	69 ± 2	50 ± 2***	72 ± 2	47 ± 1***
	Stride length right (mm)	65 ± 3	60 ± 2	62 ± 2	50 ± 2***	69 ± 2	49 ± 1***	74 ± 1	46 ± 1***
	Toespan left (mm)	8.51 ± 0.18	8.44 ± 0.19	8.48 ± 0.24	8.26 ± 0.17	7.64 ± 0.2	7.91 ± 0.16	8.13 ± 0.12	8.26 ± 0.14
	Toespan right (mm)	8.2 ± 0.22	8.14 ± 0.25	8.77 ± 0.15	7.9 ± 0.17**	7.89 ± 0.11	7.73 ± 0.19	7.3 ± 0.25	7.9 ± 0.17
	Width (mm)	26 ± 1	26 ± 0.4	29 ± 1	28 ± 0.4	29 ± 0.5	28 ± 1	29 ± 0.4	27 ± 1*

Data are presented as mean ± S.E.M. Statistical significance was determined with the two-tailed Student's *t*-test. \**p* < 0.05, \*\**p* < 0.01, \*\*\**p* < 0.001. W, wild type; HET, heterozygous.

were shielded with cardboard to prevent the mice from escaping. Testing commenced by placing an animal in the middle of the beam. The number of segments crossed (four-paw criterion), the latencies before falling, and the number of falls were measured for four trials with a cut-off period of 1 min per trial and an intertrial interval of 10 min.

#### *Accelerating rotarod*

Equilibrium, balance, and motor coordination were tested on an accelerating rotarod apparatus (Panlab, Barcelona, Spain). After two acclimatization trials with a maximum duration of 2 min each at a constant speed (4 rpm), each mouse was placed on the rotating rod for four test trials, during which the rotation speed gradually increased from 4 to 40 rpm (intertrial interval: 1 min). The time an animal remained on the rotating rod was measured during the test trials with a cut-off period of 5 min per trial.

#### *Tissue sampling and embedding*

Tau 58/4 and WT mice were anesthetized and transcardially perfused with saline. Spinal cord tissue was removed and cut into cervical, thoracic, lumbar, and sacral segments. Sciatic nerves and EDL muscles were also collected. For immunohistochemistry, spinal cord tissue ( $n = 8$ ) was formalin fixed and embedded in paraffin. Spinal cord tissue ( $n = 3$ ), left sciatic nerve ( $n = 5$ ), and left EDL muscle ( $n = 3-5$ ) were put in 4% PFA in PBS for 1 day, dehydrated with 25% sucrose in PBS overnight at 4°C and then frozen at -50°C. For neuromuscular junction innervation analysis, right EDL muscle ( $n = 3-4$ ) was snap frozen in 2-methylbutane, which was kept on dry ice (-40°C) and then stored at -80°C.

For electron microscopy, the right sciatic nerve ( $n = 5$ ) was cut into 2 mm-long pieces, and fixed with 2% PFA and 2.5% glutaraldehyde in 0.1 M PHEM buffer (20 mM PIPES, 50 mM HEPES, pH 6.9, 20 mM EGTA, 4 mM MgCl<sub>2</sub>) at room temperature [22] for 3 h. Samples were washed 3 times with 0.1 M PHEM buffer before being post-fixed in 1% osmium tetroxide and 1% potassium ferricyanide in 0.1 M PHEM buffer at 4°C for 90 min. Samples were then embedded in Epon resin as previously described [23].

#### *Immunohistochemistry*

Coronal sections of thoracic spinal cord and sagittal sections of sacral spinal cord (5 μm, paraffin-embedded) of Tau 58/4 mice at the age of 6 and 12

months were cut for immunohistochemical staining. The sections were firstly deparaffinized in xylene and ethanol. The sections were subsequently pre-incubated in 1% H<sub>2</sub>O<sub>2</sub> for 30 min. After washing in TBS, the sections were blocked for 30 min with 4% normal swine serum in TBS + 1% bovine serum albumin (BSA). Sections were then incubated at 4°C overnight with primary antibody (AT8, 1:10000, produced by Institute Born-Bunge, University of Antwerp) in TBS + 1% BSA. After TBS washing, the sections were incubated with biotinylated anti-mouse IgG (1:200, Amersham, RPN1001) in TBS + 1% BSA at room temperature for 30 min. Next, all the sections were washed with TBS and incubated in avidin-biotin-peroxidase complex (Vectastain ABC kit, Vector Laboratories, PK-6100) for 30 min and visualized with 3, 3'-diaminobenzidine (DAB, Sigma, D-5637).

Coronal sections of the lumbar spinal cord (14 μm for sections on glass slides, 40 μm for free floating tissue) of Tau 58/4 and WT mice at the age of 3, 9, and 12 months were pre-incubated in 0.3 % H<sub>2</sub>O<sub>2</sub> in PBS for 30 min (only for light microscopy). Then the sections were blocked with 10 % normal serum. Sections were incubated overnight at room temperature with the primary antibodies: NeuN (1:500, Abcam, EPR12763), AT8 (1:10000, Antwerp), Mac-2 (1:1000, Cedarlane, CL8942AP), GFAP (1:1000, DAKO, Z0334). After PBS washing, for light microscopy, sections were incubated with biotinylated secondary antibodies for 1 h (goat anti-rabbit IgG, 1:400, Vector Laboratories, BA-1000; rabbit anti-rat IgG, 1:400, Vector Laboratories, BA-4001; horse anti mouse IgG, 1:400, Vector Laboratories, BA-2000) followed by addition of the avidin-biotin-peroxidase complex (Vector Laboratories, PK-6100) for 30 min and visualized with DAB. The sections were mounted with Depex (Sigma, 06522). For fluorescence microscopy, sections were incubated in donkey anti-rabbit Alexa 488 (1:400, ThermoFisher, A-21206) and donkey anti-rat Cy3 (1:400, JIR, 712-165-150). The sections were mounted with Mowiol (Calbiochem, 475904).

#### *Immunofluorescence labeling of neuromuscular junctions*

Snap frozen EDL muscle samples (100 μm for free floating tissue) of Tau 58/4 and WT mice at the age of 3, 9, and 12 months were cut using a cryostat. Muscle sections were incubated in α-bungarotoxin Alexa 594 (1:200, Molecular Probes, B13423) in PBS for 30 min, followed by 4% PFA in PBS for

10 min. The sections were then blocked with 4% BSA in PBS for 1 h. Sections were incubated in primary antibody neurofilament-M (165 kDa) (1:300, DSHB, 2H3) with 1% BSA in PBS + 0.3% Triton X-100 for 2 h. After washing in PBS, sections were incubated in donkey anti-mouse AF488 (1:400, Molecular Probes, A21202) with 1% BSA in PBS + 0.3% Triton X-100 for 1 h. After another washing step in PBS, sections were incubated in Hoechst for 3 min and mounted on slides using Mowiol (Calbiochem, 475904).

### Imaging techniques

Histochemically stained sections were imaged using a Hamamatsu Nanozoomer (Hamamatsu Photonics). Immunofluorescent stained sections were imaged using a Leica SP8 confocal (Leica Microsystems) using LASAF software. The z-maximum-intensity projection function was used to image the complete neuromuscular junctions in the muscle.

### Motor neuron counting

The number of motor neurons in the lumbar spinal cord sections of 3-, 9-, and 12-month-old WT and Tau 58/4 mice were counted after the immunostaining of NeuN ( $n = 3$ ). On both sides of the anterior ventral horn of the spinal cord, motor neurons, identified on the basis of the location and the large size of the cell body, were counted.

### Transverse area of muscle fiber measurement

Paraffin-embedded EDL muscles of 3-, 9-, and 12-month-old WT and Tau 58/4 mice were cut (5  $\mu\text{m}$ ) and stained with Hematoxylin. The sections were scanned with a Hamamatsu Nanozoomer (Hamamatsu Photonics) and the transverse area of EDL muscles was measured by ImageJ software (100–150 fibers / sample,  $n = 3–5$ ).

### Analysis of the innervation of motor endplates

After the immunofluorescence labeling of neuromuscular junctions with neurofilament and  $\alpha$ -bungarotoxin, at least 90 neuromuscular junctions per animal ( $n = 3–4$ ) were imaged and quantified. The innervation status of the neuromuscular junction was evaluated by categorizing them as fully innervated when there was complete overlap between the two labels, partially innervated when neurofilament was partially absent at the synaptic junction or denervated

in case neurofilament was completely absent at the synaptic junction.

### Analysis of axon and myelin structure

Epon-resin-embedded samples were cut into semithin (100 nm) and ultrathin sections (70 nm) using a LEICA ultramicrotome UC7. Semithin sections were colored with toluidine blue and imaged using light microscopy before measuring the diameters of axons. The inner area of axons was measured in Image J, then the diameter was calculated and then the average diameters was extrapolated. Approximately 650–1100 axons were quantified for each sample ( $n = 3$ ).

For electron microscopy, ultrathin sections were stained as previously described [23] and examined in an 80-kV transmission electron microscope (TEM, CM100; FEI). Three independent grids (100 axons/grids) were used to assess the number of degeneration axons in each individual mouse. The g-ratio of axons with intact myelin were assessed. The g-ratio [diameter (axon) / diameter (axon + surrounding myelin)] were also calculated using Image J. Approximately 60–150 fibers was measured per animal ( $n = 4$ ).

### Statistical analysis

For the statistical analysis, SPSS version 20.0 and GraphPad Prism 5.0 software were used with the probability level set at 95%. For comparison between two groups, Student's  $t$ -test, and non-parametric Mann-Whitney test were used. For comparison of multiple groups, Two-way RM-ANOVA test was performed with a Bonferroni *post hoc* test. The data was considered statistical significant as  $*p < 0.05$ ,  $**p < 0.01$ , and  $***p < 0.001$ . In the figures, the  $p$ -value of the analysis is shown.

## RESULTS

### Tau 58/4 mice show deteriorating motor dysfunction during aging

To evaluate the coordination of motor function, we examined Tau 58/4 and WT mice in the hindlimb clasping test, gait analysis, stationary beam test, and rotarod test at the age of 3-, 6-, 9-, and 12 months (data listed in Table 1). The degree of hindlimb clasping in mice, when suspended by the tail, is used as an

indicator of the severity of motor dysfunction [24, 25]. WT mice at all indicated ages and Tau 58/4 mice at young ages (i.e., 3 and 6 months) showed a normal extension reflex of the hindlimbs. Tau 58/4 mice of 9 and 12 months old showed typical hindlimb clasp behavior (Fig. 1A). Gait is a general indicator of coordination and muscle function [26]. Gait analysis indicated that the stride length in Tau 58/4 animals is shorter than that in WT control animals. A decrease in the stride length was observed bilaterally, with a significant shorter length visible from 6 months on in the Tau 58/4 strain (Fig. 1B). The stationary beam test was used to detect balance and coordination abnormalities. Tau 58/4 mice of 9 and 12 months old remained significantly shorter on the beam. Tau 58/4 mice of all ages covered a significantly lower number of beam segments, and Tau 58/4 mice of 3, 9, and 12 months old had a significantly higher number of falls, compared to WT animals (Fig. 1C-E). Motor neuron performance and equilibrium were analyzed using an accelerating rotarod (Fig. 1F). In all age groups, significant differences between Tau 58/4 and WT animals were observed for the fourth trial (T4). From the age of 9 months on, significant differences were found for all trials performed. Also, from the age of 3 months, the learning curves differed significantly between Tau 58/4 and WT animals, with the HET animals exhibiting a much flatter learning curve. However, the results found in the rotarod experiment are possibly confounded by the agitated and stressed behavior observed in the Tau 58/4 animals, which resulted in early termination of a trial due to the jumping of the rotarod. This behavior was only this pronounced in the rotarod experiment and did not result in the early termination of the other motor experiments described above.

#### *Human Tau transgenic protein is expressed in the motor neurons of Tau 58/4 mice*

In order to investigate the relationship between motor dysfunction and tauopathy in Tau 58/4 mice, we determined tauopathy in the spinal cord and sciatic nerve of Tau 58/4 mice. AT8 antibody, which is specific for the phospho-tau residues Ser202, and Thr205, was used for immunohistochemical staining. The staining was performed on transverse sections of thoracic spinal cord and sagittal sections of the sacral spinal cord of Tau 58/4 mice at 6 months and 12 months (Fig. 2A). In 6-month-old Tau 58/4 mice, phosphorylated tau has mainly accumulated in the axonal processes. At the age of 12 months, the

expression of phosphorylated tau was increased and was also observed in the somatic compartments of motor neurons of the ventral horn (Fig. 2A). To detect the accumulation of tau-induced neuronal loss, the numbers of motor neurons were counted in the lumbar spinal cord of Tau 58/4 and WT mice at the age of 3, 9, and 12 months. No significant differences in motor neuron numbers were observed between Tau 58/4 and WT mice at all ages (Fig. 2B, C). In the sciatic nerve, enhanced expression of AT8 was observed in 9-month-old Tau 58/4 mice but not in WT mice (Fig. 2D).

#### *Tau 58/4 mice show muscle hypotrophy during aging*

To investigate the development of muscular atrophy, transverse sections of EDL muscles of WT and Tau 58/4 mice were stained with hematoxylin. Transverse areas were measured and grouped into separate regions according to size (Fig. 3A, B). The percentage of muscle fiber numbers in different regions was compared between WT and Tau 58/4 mice. At the age of 3 months, the distribution of fiber size in WT and Tau 58/4 mice is similar. At the age of 12 months, 94.5 % fibers of Tau 58/4 mice belong to smaller area regions (i.e., fiber area < 150  $\mu\text{m}^2$ ), compared to WT mice, which indicated hypotrophy of muscle in Tau 58/4 mice (Fig. 3A, B). The average area of muscular fibers was also compared between WT and Tau 58/4 mice at different ages. At the age of 3 and 9 months, no significant differences were observed. During aging, the average transverse area of EDL fibers in 12-month-old Tau 58/4 mice was significantly smaller than that of WT mice (Fig. 3C).

#### *Tau 58/4 mice show progressive neuromuscular junction denervation during aging*

In order to investigate whether the axonal terminals at the neuromuscular junction are early targets for lower motor neuron pathology in Tau 58/4 mice, we analyzed the integrity of the neuromuscular junction in EDL muscle from hindlimbs. Based on the innervation of the motor endplate, neuromuscular junctions were grouped into fully innervated, partially innervated, and denervated junctions (Fig. 4A). At 3 months, the innervation of the motor endplate in WT and Tau 58/4 mice was not significantly different. In 12-month-old Tau 58/4 mice, there was widespread endplate denervation. This was evident by degeneration of presynaptic motor nerve terminals that had

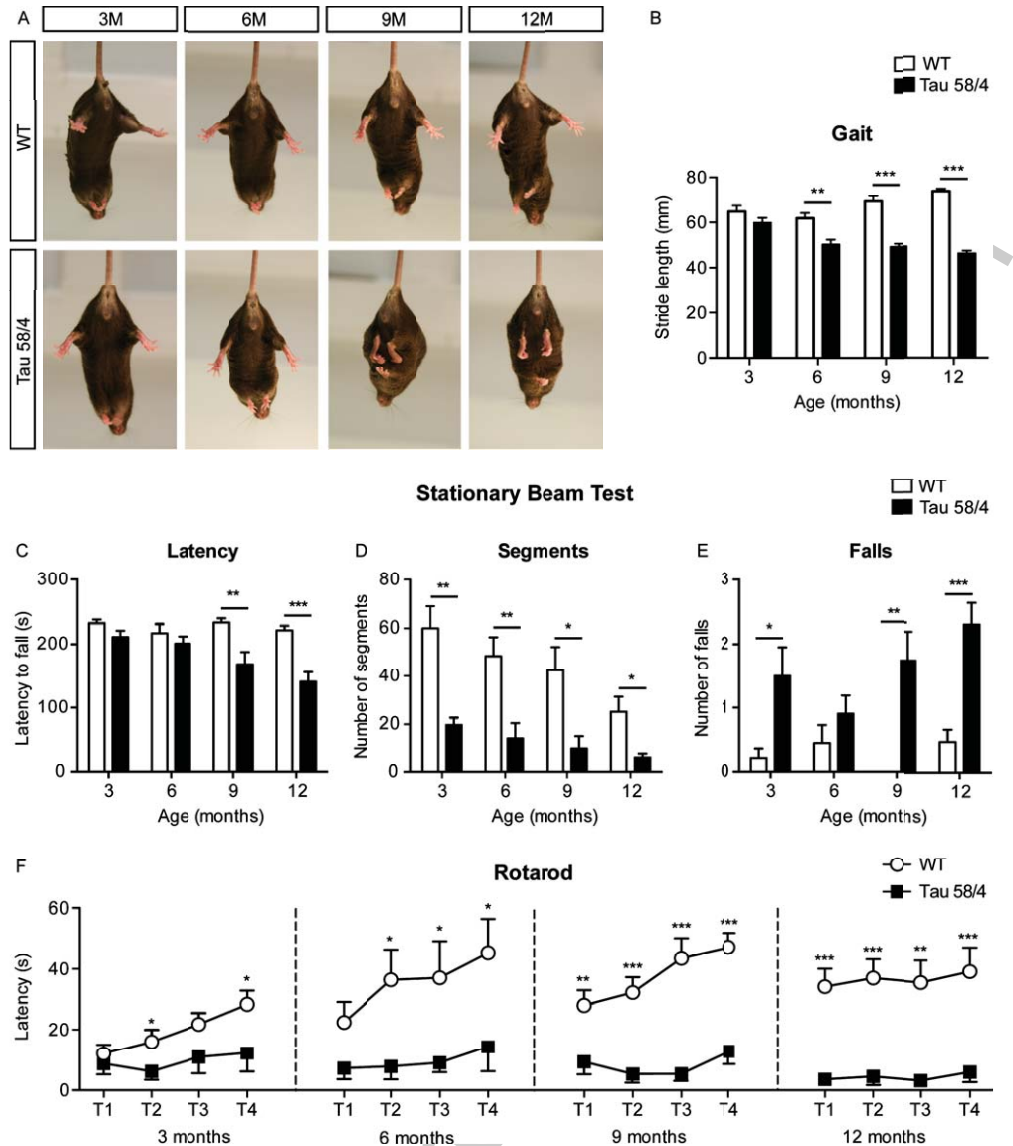


Fig. 1. Motor dysfunction deteriorates in Tau 58/4 mice during aging. A) Representative postures of Tau 58/4 and wild-type (WT) mice in the hindlimb clasp test at the age of 3, 6, 9, and 12 months. WT mice of all ages and Tau 58/4 mice of 3 and 6 months old showed a normal extension reflex in the hindlimbs. However, hindlimb clasp was observed in Tau 58/4 HET animals at the age of 9 and 12 months. B) Gait analysis was performed in Tau 58/4 mice and WT mice at the age of 3, 6, 9, and 12 months. Tau 58/4 mice of 6, 9, and 12 months old showed a shorter stride length compared to WT control mice. Indicated in this figure is the stride length of the right side of the animal and no significant difference was observed between the right and the left stride lengths. Most prominent differences were observed in 12-month-old mice ( $p < 0.001$ ). C-E) Stationary beam testing was performed in Tau 58/4 mice and WT mice at the age of 3, 6, 9, and 12 months. Tau 58/4 mice scored inferior for all measured parameters (the number of covered segments and falls and the duration until the first fall), indicating an impairment in motor function and equilibrium. For Tau 58/4 animals, a significant reduction was observed in the number of covered segments of all age groups [3 months ( $p = 0.002$ ), 6 months ( $p = 0.003$ ), 9 months ( $p = 0.010$ ), and 12 months ( $p = 0.010$ )]. The number of falls from the beam was increased in Tau 58/4 animals as well [3 months ( $p = 0.022$ ), 9 months ( $p = 0.002$ ), and 12 months ( $p < 0.001$ )]. The latency to fall was significant shorter in Tau 58/4 animals of 9 months old ( $p = 0.007$ ) and for mice aged 12 months ( $p < 0.001$ ). F) Rotarod results for Tau 58/4 and WT mice at the age of 3, 6, 9, and 12 months. WT animals scored significantly better in the test phase (4 trials, T1, T2, T3, and T4, with a 5-min acceleration to 40 rpm). 3 months: WT  $n = 9$ , HET  $n = 10$ ; 6 months: WT  $n = 11$ , HET  $n = 11$ ; 9 months: WT  $n = 11$ , HET  $n = 12$ ; 12 months: WT  $n = 15$ , HET  $n = 16$ ; Mean  $\pm$  SEM; All age groups: Two-way RM-ANOVA with Bonferroni *post hoc* comparison; Each individual time point: Student's *t*-test, two-tailed, \* $p < 0.05$ ; \*\* $p < 0.01$ , and \*\*\* $p < 0.001$ .



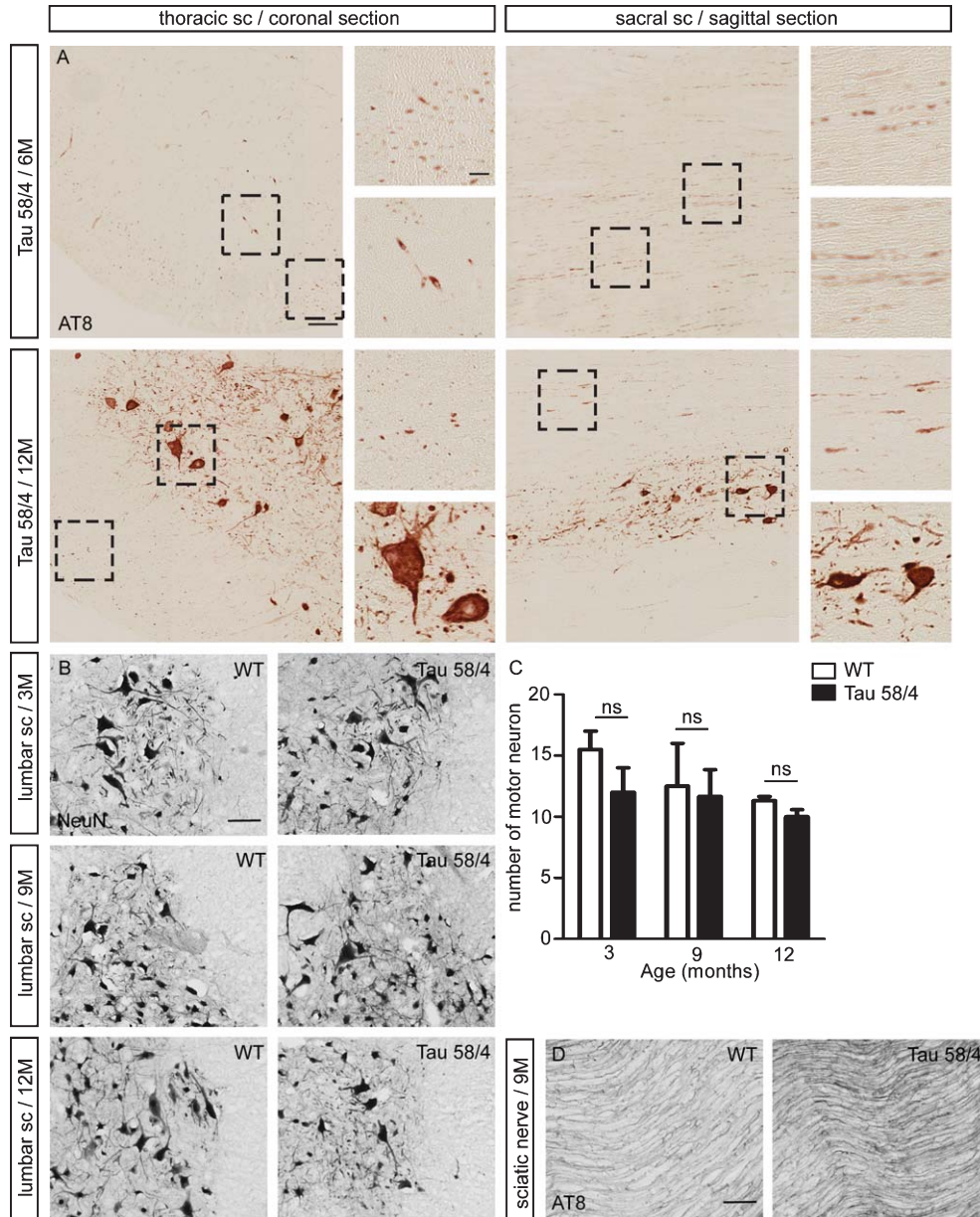


Fig. 2. Tau pathology develops in the spinal cord of Tau 58/4 mice with aging. A) The spinal cord of Tau 58/4 mice at the age of 6 or 12 months was immunostained with AT8 antibody, specific for human mutant tau. The expression of AT8 increased with aging. Magnified pictures show tau pathology in the gray matter and white matter of thoracic spinal cord and sacral spinal cord. B) The spinal cord of WT and Tau 58/4 mice at 3, 9, and 12 months old was immunostained with NeuN. Motor neurons in the anterior horn were clearly identified. C) The number of motor neurons in the lumbar spinal cord of WT (white bar) and Tau (black bar) was quantified at the age of 3, 9, and 12 months. There were no significant differences of motor neuron numbers between WT and Tau 58/4 mice at different ages ( $n=3$ , Mean  $\pm$  SEM, Mann-Whitney test, two-tailed,  $*p < 0.05$ ). D) The sciatic nerve of 9-month-old WT and Tau 58/4 mice was immunostained with AT8. The expression of phosphorylated tau was higher in Tau 58/4 mice. Scale bars: A = 100  $\mu$ m, Magnification = 10  $\mu$ m; B, D = 40  $\mu$ m.

472 either entirely or partially disappeared from the post-  
 473 synaptic motor endplate. Upon aging, there was a  
 474 decreased percentage of fully innervated endplates  
 475 and accordingly an increased percentage of partially  
 476 or completely denervated endplates in Tau 58/4 mice

(Fig. 4B). The development of neuromuscular junction  
 477 denervation during aging was accompanied by  
 478 deteriorating motor dysfunction, which indicated the  
 479 distal axonal pathology could be a cause of motor  
 480 deficit of Tau 58/4 mice.  
 481

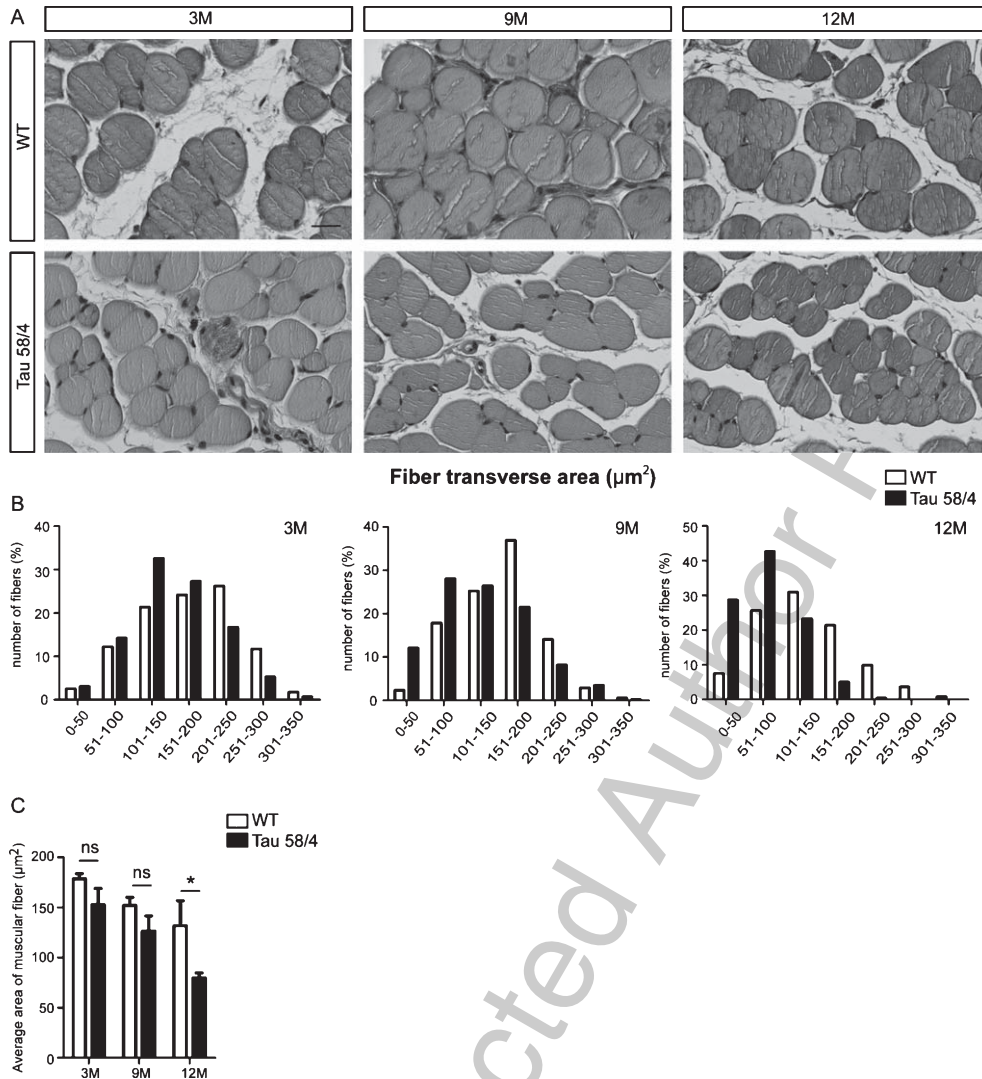


Fig. 3. Muscle hypotrophy in Tau 58/4 mice. A) Hematoxylin staining on transverse sections of extensor digitorum longus (EDL) muscle from 3-, 9-, and 12-month-old WT and Tau 58/4 mice. B) Quantification of transverse area of the muscular fiber of 3-, 9-, and 12-month-old WT (white bar) and Tau 58/4 mice (black bar). At the age of 3 months, the distribution of fiber areas in EDL was similar between WT and Tau 58/4 mice. At the age of 9 months and 12 months, there were significantly reduced proportions of largest muscle fibers in Tau 58/4 mice, compared to WT mice ( $n = 3-5$ ). C) Average area of the transverse section of EDL was compared between WT and Tau 58/4 mice at the age of 3, 9, and 12 months ( $n = 3-5$ , Mean  $\pm$  SEM, Mann-Whitney test, two-tailed,  $*p < 0.05$ ). Scale bar: A = 40  $\mu\text{m}$ .

482 *Ultrastructural analyses reveal axonal*  
483 *degeneration in the sciatic nerve of Tau 58/4 mice*

484 In order to study the structural alterations in myelinated axons of Tau 58/4 mice of 12 months old,  
485 we quantified the axon diameter of transverse sections of sciatic nerve stained with toluidine blue  
486 (Fig. 5A-D). The average diameter of axons in sciatic nerve was significantly decreased in Tau 58/4  
487 mice (Fig. 5B). The histogram of diameter distribution showed that 89.8% axons of Tau 58/4 mice had  
488  
489  
490  
491

a small size ( $< 4 \mu\text{m}$ ), whereas in WT mice the percentage was 75.0% (Fig. 5C). We classified the axons  
492 larger than the average diameter of WT mice as “large axons”, and those smaller than the average diameter  
493 as “small axons”. Tau 58/4 mice had a significantly higher percentage of small axons and a significantly  
494 lower percentage of large axons, compared to WT mice (Fig. 5D). To evaluate the axonal degeneration  
495 of Tau 58/4 mice, we examined the sciatic nerve morphology of WT and Tau 58/4 mice at the age  
496 of 12 months using electron microscopy (Fig. 5E).  
497  
498  
499  
500  
501  
502

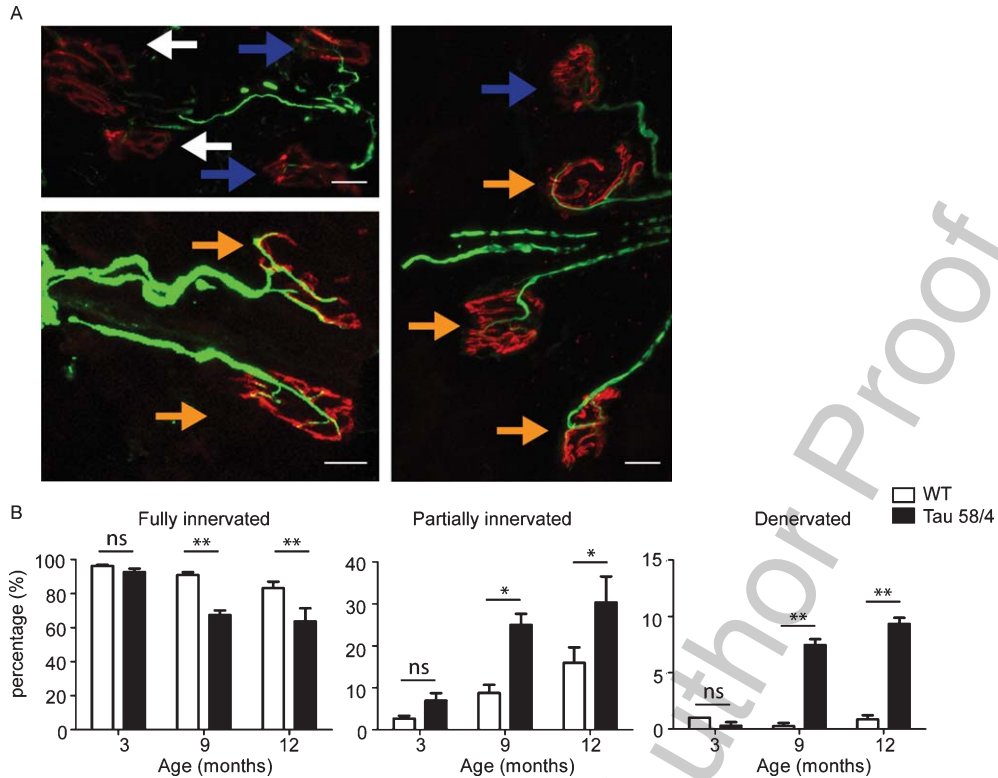


Fig. 4. Expression of human mutant tau protein leads to neuromuscular junction (NMJ) denervation in Tau 58/4 mice. A The neuromuscular junctions of EDL muscle were immunostained with 165 kDa neurofilament (green) to reveal pre-synaptic axons and motor nerve terminals and labeled with  $\alpha$ -bungarotoxin (red) to show post-synaptic motor endplates. Arrows indicate examples of fully innervated (orange arrows), partially innervated (blue arrows), and denervated (white arrows) NMJs. B) Quantification of percentages of fully innervated, partially innervated, and denervated NMJs, comparing 3-, 9-, and 12-month-old WT (white bar) and Tau 58/4 mice (black bar). At the age of 3 months, the percentage of innervated NMJs is similar between WT and Tau 58/4 mice. There is a significantly reduced percentage of fully innervated NMJs and a significantly higher percentage of partially innervated and denervated NMJs in Tau 58/4 mice at the age of 9 and 12 months. (>90 NMJ / animal,  $n = 3-4$ , Mean  $\pm$  SEM, Mann-Whitney test, two-tailed, \* $p < 0.05$ , \*\* $p < 0.01$ ). Scale bar: A = 20  $\mu$ m.

503 We observed proliferation of nonmyelinated axons  
 504 surrounded by Schwann cells (white arrow) in the  
 505 sciatic nerve of Tau 58/4 mice. We compared the  
 506 myelin sheath thickness using the g-ratio, the numerical  
 507 ratio between the diameter of the axon and the  
 508 outer diameter of the myelinated fiber. Tau 58/4 mice  
 509 showed an increasing tendency in g-ratio, which was  
 510 significantly different in the axons with a diameter  
 511 of 6–8  $\mu$ m (Fig. 5F). This observation indicated  
 512 an hypomyelination of motor-related axons of Tau  
 513 58/4 mice [27]. Except the axons with intact myelin  
 514 sheath (Supplementary Figure 1A), we also observed  
 515 less electron-dense lines (black arrow) in the myelin  
 516 sheath of axons (Supplementary Figure 1B) in both  
 517 WT and Tau 58/4 mice. However, this type of axons  
 518 was more pronounced in Tau 58/4 animals. Although  
 519 this was evident, the low frequency of this type of  
 520 axons did not allow to determine whether this difference  
 521 was significant (Supplementary Figure 1C).

522 The irregular structures in the myelin sheath might  
 523 be Schmidt-Lanterman incisura, which is a funnel  
 524 tube-like cytoplasmic structure that crosses the compact  
 525 myelin and connects the Schwann cell abaxonal  
 526 cytoplasm to the adaxonal cytoplasm [28]. However  
 527 further investigation will be needed to confirm that  
 528 these structures are Schmidt-Lanterman incisures.

#### 529 *Increased glia activity in the corticospinal tract* 530 *of spinal cord in Tau 58/4 mice*

531 In order to investigate the involvement of upper  
 532 motor neurons in the lower motor neuron dysfunction  
 533 in Tau 58/4 mice, we investigated the glia activity in  
 534 the corticospinal tract of the spinal cord of Tau 58/4  
 535 mice and WT mice. Mac-2, which is a member of the  
 536 lectin family, has been observed to be upregulated in  
 537 microglia and astrocytes upon aging and pathological  
 538 conditions [29]. At the age of 9 and 12 months, we  
 539



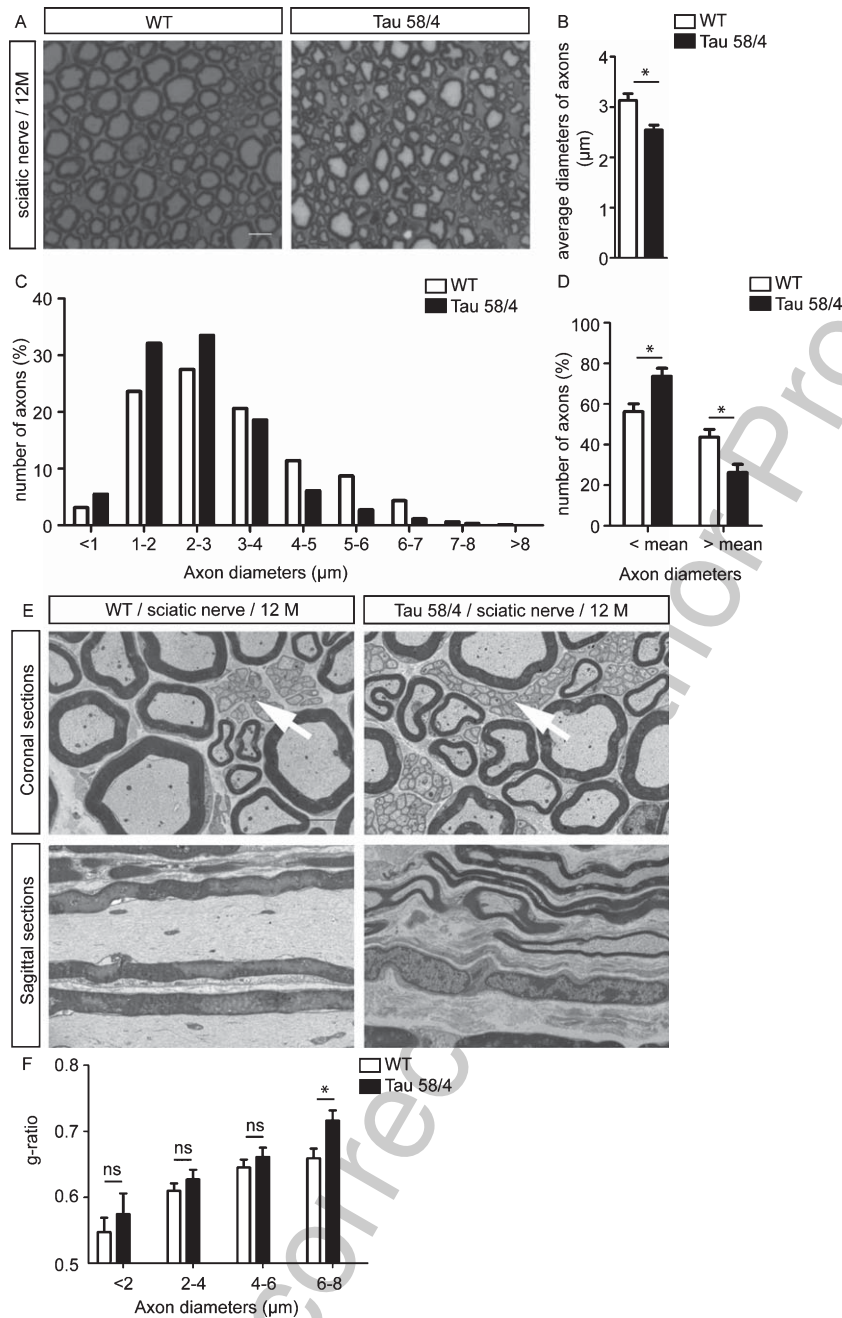


Fig. 5. Ultrastructural features of the sciatic nerve reveal axonal degeneration in Tau 58/4 mice. A) Representative light microscopy photograph of toluidine blue staining of the sciatic nerve of 12-month-old WT and Tau 58/4 mice (650–1100 axons / animal,  $n = 3$ ). B) Quantification of the average transverse diameter of axons in 12-month-old WT (white bar) and Tau 58/4 (black bar). C) The histogram of axon diameters shows more axons of Tau 58/4 mice have a small diameter ( $< 4 \mu\text{m}$ ). D) Compared to the average diameters of WT mice, axons were set as “large axons” and “small axons”. Tau 58/4 has a significantly higher percentage of small axons and a lower percentage of large axons. E) Coronal and sagittal ultrathin sections of the sciatic nerve of WT and Tau 58/4 mice at the age of 12 months (white arrows: non-myelinating axons surrounded by Schwann cells). F) Quantification of the g-ratio in the sciatic nerve of 12-month-old WT and Tau 58/4 mice (60–150 axons / animal,  $n = 5$ , Mean  $\pm$  SEM, Mann-Whitney test, two-tailed,  $*p < 0.05$ ). Scale bar: A =  $10 \mu\text{m}$ , E =  $2 \mu\text{m}$ .

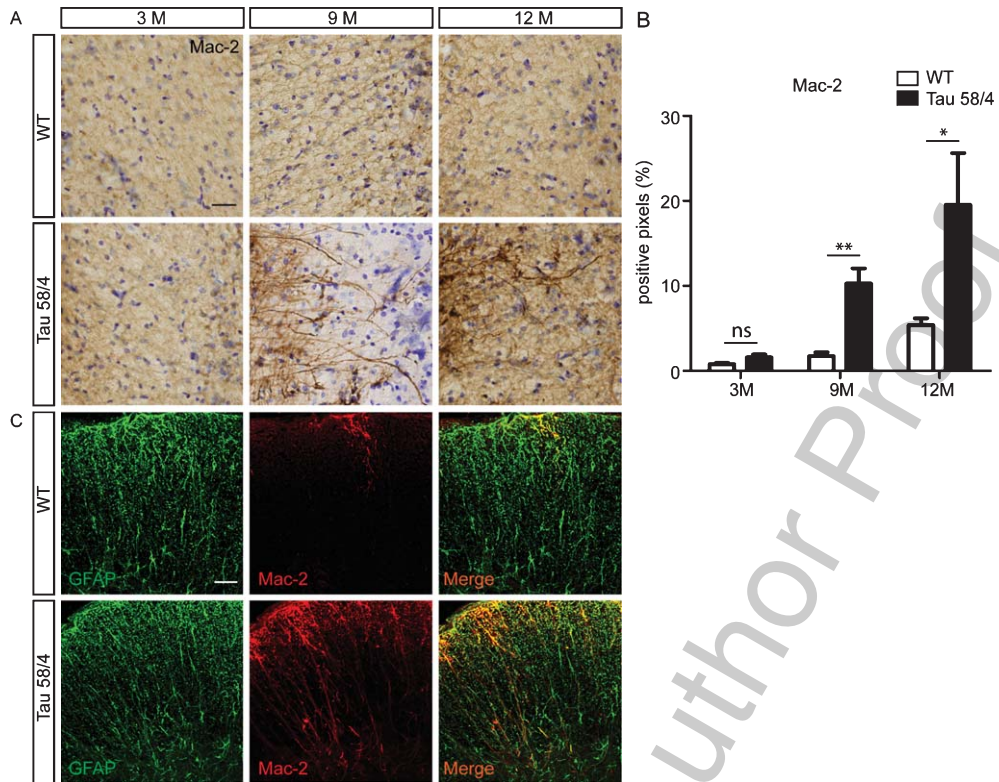


Fig. 6. Astrocyte activation in the lateral corticospinal tract in Tau 58/4 mice. A) Lumbar spinal cord sections of 3-, 9- and 12-month-old Tau 58/4 and WT mice were immunostained with Mac-2 and counterstained with Cresyl violet. Representative pictures were taken from the region of the lateral corticospinal tract. B) The percentage of positive pixels of Mac-2 in the white matter of lumbar spinal cord, and the expression of Mac-2 was significantly increased in the Tau 58/4 mice of 9- and 12 months old compared to WT ( $n = 3-5$ , Mean  $\pm$  SEM, Mann-Whitney test, two-tailed,  $*p < 0.05$ ,  $**p < 0.01$ ). C) Lumbar spinal cord sections of 12-month-old Tau 58/4 and WT mice were immunostained with GFAP and Mac-2. Co-staining were observed between GFAP and Mac-2. Scale bar: A = 25  $\mu$ m, C = 40  $\mu$ m.

in Tau 58/4 mice was significantly increased in the white matter regions (Fig. 6B). We also observed co-staining of Mac-2 and GFAP in the region of the lateral corticospinal tract (Fig. 6C), indicative of astrocyte activation in the region of corticospinal tract responding to neuronal changes.

## DISCUSSION

In this study, we investigated the motor function and pathological alterations of peripheral nerves in a novel tauopathy mouse model, the Tau 58/4 model. We observed loss of large size peripheral axons, denervation of neuromuscular junctions in 12-month-old Tau 58/4 mice as compared to control littermates. These alterations may lie at the basis of muscle hypotrophy and progressive motor impairment (Fig. 7).

In our study, the stationary beam- and rotarod tests revealed a decline in the motor function already at

the age of 3 months. However, rotarod results can be influenced by certain alterations in behavior, such as agitation [30]. Training a highly anxious and agitated animal on the rotarod is much more challenging when compared with calmer animals [31], resulting in an apparently decreased performance of animals that is unrelated to motor function, as described in the PS19 tauopathy mouse model [17]. In previous studies, it was found that rotarod experiments failed to reveal subtle motor alterations, whereas gait analysis and stationary beam tests were more sensitive [32, 33]. Based on the stationary beam tests, the apparent decline in motor functioning in Tau 58/4 mice, starts already at the early age of 3 months. Tau 58/4 mice started to show hindlimb clasping behavior at the age of 9 months, which was later than the onset of the motor coordination impairment observed in the rotarod test and stationary beam. We also observed hindlimb muscle hypotrophy at 9 months, which may explain the observed muscle weakness. Previous studies have exposed

561  
562  
563  
564  
565  
566  
567  
568  
569  
570  
571  
572  
573  
574  
575  
576  
577  
578  
579  
580  
581

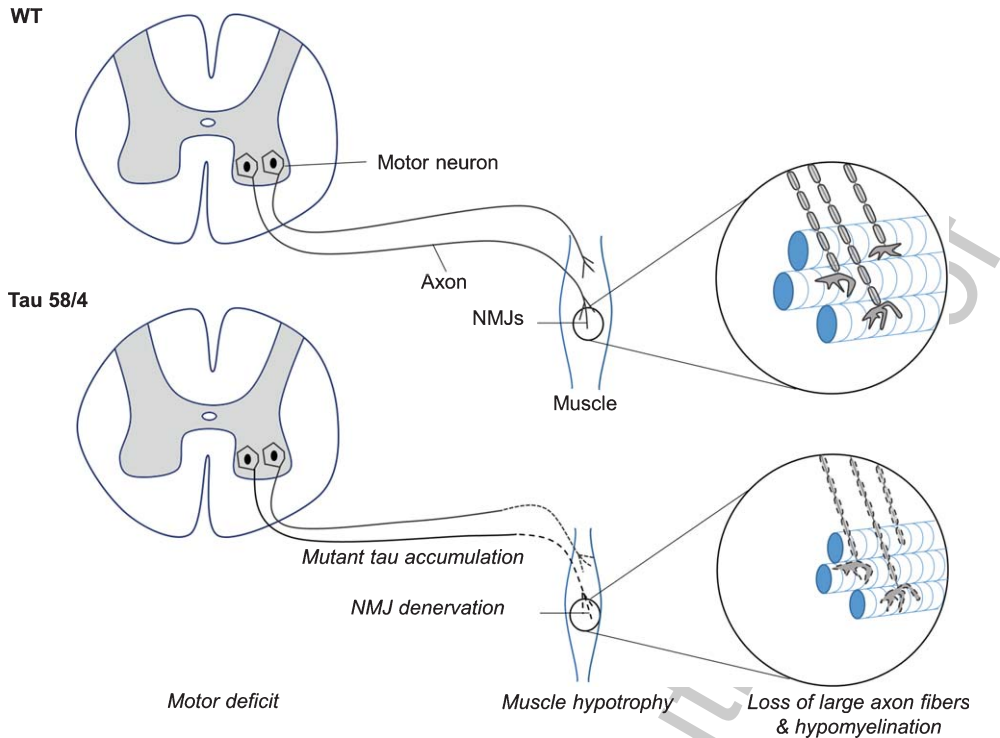


Fig. 7. A schematic representation of hypothetical mechanism for motor deficit in Tau 58/4 mice. In WT mice, motor neurons in the ventral horn of the spinal cord send axons toward the peripheral muscle. Each muscle fiber is innervated by a single motor axon branch. In Tau 58/4 mice, accumulated mutant tau in the axon terminals may induce hypomyelination, loss of large axon fibers, neuromuscular junction denervation, and muscle hypotrophy, which may be the mechanism responsible for motor deficit in Tau 58/4 mice.

582 diverse cognitive and motor phenotypes in various  
 583 transgenic tauopathy models which may well be due  
 584 to distinctive pathways of tau molecular pathogenesis  
 585 and different localization of tau pathology [34]. In  
 586 PS19 transgenic mice expressing the P301S human  
 587 T34 tau isoform driven by the mouse prion protein  
 588 (Prnp) promoter, increased hyperactivity and  
 589 nociceptive sensitivity, and decreased anxiety-like  
 590 behavior have been reported [16]. Delayed learning  
 591 and spatial memory loss have also been found  
 592 in various transgenic tauopathy mouse models [16,  
 593 35, 36]. Motor dysfunction and dystonic posture  
 594 interference are phenomena observed in transgenic  
 595 tau mouse models with aggregated mutant tau in  
 596 axons [8, 34, 37]. However, in the two previously  
 597 described P301S tauopathy mouse models [17, 38],  
 598 the motor deficits are so severe that they hinder the  
 599 age-dependent investigation of specific motor-related  
 600 functions, as paralysis occurs early in the disease. One  
 601 exception is the THY-Tau22 model with G272V and  
 602 P301S mutations, which does not display any motor  
 603 disturbance [36], although insoluble tau was early  
 604 (3 months) detected in the axon tracts. In Tau 58/4  
 605 mice, mutant tau proteins accumulate both in somata

606 and axonal compartments of motor neurons, and the  
 607 axonal distribution of mutant tau may be pivotal for  
 608 the motor impairment. Previous studies in transgenic  
 609 tau-P301L mouse models indicated that mutant tau  
 610 mainly aggregated in the soma and dendritic compart-  
 611 ments, rather than in axons. Interestingly, no axonal  
 612 dilations were observed at any age in latter model,  
 613 and it shows very weak motor symptoms accordingly  
 614 [39]. In this respect, Tau 58/4 mice represent a  
 615 straightforward neuromuscular degeneration model.

616 We observed progressive hypotrophy of muscle  
 617 fibers and denervation of the neuromuscular junction  
 618 in aging Tau 58/4 mice. At the age of 9 and 12  
 619 months, the muscle hypotrophy accompanied a further  
 620 decrease in motor dysfunction. This has also been  
 621 reported in other transgenic tauopathy mouse models  
 622 [15, 38]. In Tg30 mice (carrying tau P301S and  
 623 G272V mutations), two phases of muscular pathology  
 624 were observed. Initially, muscular hypertrophy was  
 625 observed at the age of 3 months followed by  
 626 hypotrophy at the age of 10 months. The muscle  
 627 hypertrophy at the early age was interpreted as a  
 628 compensatory mechanism for the degeneration of  
 629 the nearby muscles and protected the animals from  
 630

630 motor dysfunction until 8 months of age [8]. In Tau  
631 58/4 mice muscular hypertrophy was not observed in  
632 3-month-old animals, which may explain the rapid  
633 development of motor dysfunction in this model.  
634 Neuromuscular junction denervation has been asso-  
635 ciated with aging [40] and pathological conditions,  
636 such as contraction-induced injury [41] and neu-  
637 rodegenerative disorders [42, 43]. In Tau 58/4 mice,  
638 the development of neuromuscular junction denerva-  
639 tion occurs together with the progression of muscle  
640 hypotrophy, which is indicative for denervation-  
641 mediated atrophy.

642 Interestingly, mutant tau also accumulated in the  
643 cell body of the motor neurons at the anterior horn  
644 of the spinal cord. However, we did not observe  
645 a decrease in the number of motor neurons. This  
646 suggests that the pathology of the motor neurons  
647 follows a distal-to-proximal direction. Axon degen-  
648 eration in Tau 58/4 mice could be considered to be  
649 “dying back degeneration”, which has been described  
650 previously in chronic neurodegenerative diseases,  
651 such as amyotrophic lateral sclerosis [44], spinal  
652 muscular atrophy [45], diffuse Lewy body disease  
653 [46], and peripheral neuropathy [47]. Generally,  
654 this type of chronic axonal degeneration originates  
655 from the distal region of the axon and is followed  
656 by axon degeneration in a distal-to-proximal direc-  
657 tion. The axon subsequently undergoes a progressive  
658 fragmentation morphologically resembling Walle-  
659 rian degeneration [13]. The mechanisms underlying  
660 “dying back degeneration” are not fully under-  
661 stood, but mitochondrial dysfunction [48, 49], protein  
662 aggregation [49], synaptic pathology [50], distur-  
663 bance of axonal transport [51, 52], and abnormal  
664 activity of autophagy [53] have been previously found  
665 to be involved in the process. In Tau 58/4 mice, the  
666 neuronal accumulation of mutant tau might be a key  
667 player in axonal degeneration. In cultured neurons,  
668 aggregated tau inhibits kinesin-dependent transport  
669 of organelles, e.g. peroxisomes, mitochondria, and  
670 Golgi-derived vesicles into neurites [54]. The inhi-  
671 bition of axonal transport causes oxidative stress,  
672 reduces ATP content in synapses and leads to cellular  
673 degeneration. Tau could also impair axonal and den-  
674 dritic ATP transport and thus lead to the accumulation  
675 of A $\beta$ PP in the cell body [54, 55]. The reduction of tau  
676 expression does not influence axonal transport under  
677 physiological conditions, however, it could prevent  
678 A $\beta$  oligomers-impaired axonal motility [56].

679 In our study, we also observed axonal hypomyeli-  
680 nation in the sciatic nerve of 12-month-old Tau  
681 58/4 mice. Axonal demyelination in sciatic nerve

682 has been observed under various pathological condi-  
683 tions including physical injury, chronic inflammatory  
684 polyneuropathy, and diabetes [57]. A previous study  
685 in myelin-deficient Trembler mice showed a reduc-  
686 tion in the rate of slow axonal transport and a slower  
687 regeneration rate in demyelinated sciatic nerve [58].  
688 Tau protein plays an important role in the structure  
689 and function of myelin. In a recent study, enhanced  
690 degenerating, demyelinated fibers and motor impair-  
691 ment in the sciatic nerve of aged Tau  $-/-$  mice  
692 was observed [27]. Abnormal phosphorylation of  
693 tau was associated with both neuronal and axonal  
694 loss in animal models of experimental autoimmune  
695 encephalomyelitis as well as in human multiple scler-  
696 osis [59, 60]. Here, our observations indicate that  
697 hyperphosphorylation and accumulation of tau may  
698 be associated with axonal degeneration in the periph-  
699 eral nervous system.

700 We observed the proliferation of non-myelinating  
701 axon surrounded by Schwann cell in the sciatic nerve  
702 of 12-month-old Tau 58/4 mice. Schwann cells play  
703 an important role in modulation and regenerative sup-  
704 port of peripheral axons [58, 61]. Regeneration of  
705 non-myelinated axons was also observed after the  
706 injury of mammalian peripheral nerve [62]. Previ-  
707 ous studies report the non-myelinating Schwann cells  
708 distal to nerve injury undergo a large scale change in  
709 gene expression, which alters the Schwann cell func-  
710 tion from the maintenance of axonal ensheathment to  
711 the support of axonal regeneration [63, 64]. Here, the  
712 proliferation of non-myelinating Schwann cells may  
713 imply an attempt for repair.

714 Astrocytes play an important role in axon guidance  
715 during development and repair [65]. Previous studies  
716 have reported progressive astrogliosis and microglia  
717 activation in the brain of transgenic Tau mice  
718 [17, 66]. Here, we for the first time observed increased  
719 Mac-2 expression by astrocytes in the region of the  
720 lateral corticospinal tracts in the spinal cord. Mac-2  
721 is a marker associated with the degradation of myelin  
722 by microglia, the brain’s professional phagocyte, [67]  
723 and nonprofessional phagocytes, e.g., astrocyte [68],  
724 Schwann cells [69]. The increased number of phago-  
725 cytic astrocytes might be a response in respect of  
726 clearance of neuronal debris, which may indicate  
727 an increased axonal stress from corticospinal tracts  
728 or lower motor neurons in Tau 58/4 mice. Future  
729 research may aim at the elucidation of the underlying  
730 mechanisms.

731 In this study, we show that accumulation of human  
732 tau in axons and cell bodies of motor neurons leads  
733 to axonal atrophy and hypomyelination, followed by

denervation of neuromuscular junctions and muscular atrophy, leading to impairment of motor functions. The underlying mechanisms of motor deficits in Tau 58/4 mice might be responsible for motor signs observed in some human tauopathies.

## ACKNOWLEDGMENTS

We acknowledge Dr. Matthias Staufenbiel for sharing the Tau 58/4 mice line, Prof. Roy Weller, Dr. Wilfred den Dunnen, Dr. Mario Mauthe, Dr. Inge Zijdwind, and Zhuozhao Zhan for useful discussions, and Klaas Sjollema for technical assistance in confocal microscopy. This work was supported by China Scholarship Council (Grant number 201206160050, 2015506610008), Memorable grant from Deltaplan Dementie (Grant number 686180), the Research Foundation-Flanders (FWO), Interuniversity Attraction Poles (IAP) Network P7/16 of the Belgian Federal Science Policy Office, agreement between Institute Born-Bunge and University of Antwerp, the Medical Research Foundation Antwerp, the Thomas Riellaerts research fund, Neurosearch Antwerp, the Belgian Alzheimer Research Foundation (SAO-FRA), and the Alzheimer Research Center of the University Medical Center Groningen (UMCG).

Authors' disclosures available online (<http://j-alz.com/manuscript-disclosures/16-1206r1>).

## SUPPLEMENTARY MATERIAL

The supplementary material is available in the electronic version of this article: <http://dx.doi.org/10.3233/JAD-161206>.

## REFERENCES

- [1] Lee VM-Y, Goedert M, Trojanowski JQ (2001) neurodegenerative tauopathies. *Annu Rev Neurosci* **24**, 1121-1159.
- [2] Scarmeas N, Hadjigeorgiou GM, Papadimitriou A, Dubois B, Sarazin M, Brandt J, Albert M, Marder K, Bell K, Honig LS, Wegesin D, Stern Y (2004) Motor signs during the course of Alzheimer disease. *Neurology* **63**, 975-982.
- [3] Gianutsos JG, Golomb J (1997) Motor/psychomotor dysfunction in normal aging, mild cognitive decline, and early Alzheimer's disease: Diagnostic and differential diagnostic features. *Int Psychogeriatrics* **9**, 307-316.
- [4] Williams DR (2006) Tauopathies: Classification and clinical update on neurodegenerative diseases associated with microtubule-associated protein tau. *Intern Med J* **36**, 652-660.
- [5] Karakaya T, Fußer F, Prvulovic D, Hampel H (2012) Treatment options for tauopathies. *Curr Treat Options Neurol* **14**, 126-136.
- [6] Nath U, Ben-Shlomo Y, Thomson RG, Lees AJ, Burn DJ (2003) Clinical features and natural history of progressive supranuclear palsy: A clinical cohort study. *Neurology* **60**, 910-916.
- [7] Chiba S, Takada E, Tadokoro M, Taniguchi T, Kadoyama K, Takenokuchi M, Kato S, Suzuki N (2012) Loss of dopaminoreceptive neuron causes L-dopa resistant parkinsonism in tauopathy. *Neurobiol Aging* **33**, 2491-2505.
- [8] Audouard E, Van Hees L, Suain V, Yilmaz Z, Poncelet L, Leroy K, Brion JP (2015) Motor deficit in a tauopathy model is induced by disturbances of axonal transport leading to dying-back degeneration and denervation of neuromuscular junctions. *Am J Pathol* **185**, 2685-2697.
- [9] Iqbal K, Del C, Alonso A, Chen S, Chohan MO, El-Akkad E, Gong CX, Khatoon S, Li B, Liu F, Rahman A, Tanimukai H, Grundke-Iqbal I (2005) Tau pathology in Alzheimer disease and other tauopathies. *Biochim Biophys Acta* **1739**, 198-210.
- [10] Ingram EM, Spillantini MG (2002) Tau gene mutations: Dissecting the pathogenesis of FTDP-17. *Trends Mol Med* **8**, 555-562.
- [11] Boutajangout A, Authelat M, Blanchard V, Touchet N, Tremp G, Pradier L, Brion J-P (2004) Characterisation of cytoskeletal abnormalities in mice transgenic for wild-type human tau and familial Alzheimer's disease mutants of APP and presenilin-1. *Neurobiol Dis* **15**, 47-60.
- [12] Zhang B, Maiti A, Shively S, Lakhani F, McDonald-Jones G, Bruce J, Lee EB, Xie SX, Joyce S, Li C, Toleikis PM, Lee VM-Y, Trojanowski JQ (2005) Microtubule-binding drugs offset tau sequestration by stabilizing microtubules and reversing fast axonal transport deficits in a tauopathy model. *Proc Natl Acad Sci U S A* **102**, 227-231.
- [13] Lingor P, Koch JC, Tönges L, Bähr M (2012) Axonal degeneration as a therapeutic target in the CNS. *Cell Tissue Res* **349**, 289-311.
- [14] Lee VM-Y, Kenyon TK, Trojanowski JQ (2005) Transgenic animal models of tauopathies. *Biochim Biophys Acta* **1739**, 251-259.
- [15] Lewis J, McGowan E, Rockwood J, Melrose H, Nacharaju P, Van M, Gwinn-hardy K, Murphy MP, Baker M, Yu X, Duff K, Hardy J, Corral A, Lin W, Yen S, Dickson DW, Davies P, Hutton M (2000) Neurofibrillary tangles, amyotrophy and progressive motor disturbance in mice expressing mutant (P301L) tau protein. *Nat Genet* **25**, 402-405.
- [16] Takeuchi H, Iba M, Inoue H, Higuchi M, Takao (2011) P301S mutant human tau transgenic mice manifest early symptoms of human tauopathies K, Tsukita K, Karatsu Y, Iwamoto Y, Miyakawa T, Suhara T, Trojanowski JQ, Lee VM-Y, Takahashi R with dementia and altered sensorimotor gating. *PLoS One* **6**, e21050.
- [17] Yoshiyama Y, Higuchi M, Zhang B, Huang SM, Iwata N, Saido T, Maeda J, Suhara T, Trojanowski JQ, Lee VMY (2007) Synapse loss and microglial activation precede tangles in a P301S tauopathy mouse model. *Neuron* **53**, 337-351.
- [18] Ishihara T, Hong M, Zhang B, Nakagawa Y, Lee MK, Trojanowski JQ, Lee VM-Y (1999) Age-dependent emergence and progression of a tauopathy in transgenic mice overexpressing the shortest human tau isoform. *Neuron* **24**, 751-762.
- [19] Götz J, Chen F, Dorpe J, van, Nitsch RM (2001) Formation of neurofibrillary tangles in P301L tau transgenic mice induced by Aβ42 fibrils. *Science* **293**, 1491-1495.
- [20] Andrä K, Abramowski D, Duke M, Probst A, Wiederhold KH, Bürki K, Goedert M, Sommer B, Staufenbiel M (1996) Expression of APP in transgenic mice:



- 848 A comparison of neuron-specific promoters. *Neurobiol*  
849 *Aging* **17**, 183-190.
- 850 [21] Lüthi A, Van der Putten H, Botteri FM, Mansuy IM, Meins  
851 M, Frey U, Sansig G, Portet C, Schmutz M, Schröder  
852 M, Nitsch C, Laurent JP, Monard D (1997) Endogenous  
853 serine protease inhibitor modulates epileptic activity and  
854 hippocampal long-term potentiation. *J Neurosci* **17**, 4688-  
855 4699.
- 856 [22] Schliwa M, Van Blerkom J (1981) Structural interaction of  
857 cytoskeletal components. *J Cell Biol* **90**, 222-235.
- 858 [23] Verheije MH, Raaben M, Mari M, Te Lintelo EG, Reg-  
859 giori F, Van Kuppeveld FJM, Rottier PJM, De Haan  
860 CAM (2008) Mouse hepatitis coronavirus RNA replication  
861 depends on GBF1-mediated ARF1 activation. *PLoS Pathog*  
862 **4**, e1000088.
- 863 [24] Lei P, Ayton S, Moon S, Zhang Q, Volitakis I, Finkelstein  
864 DI, Bush AI (2014) Motor and cognitive deficits in aged tau  
865 knockout mice in two background strains. *Mol Neurode-*  
866 *gener* **9**, 29.
- 867 [25] Zhu J, Li Y, Wang Z, Jia W, Xu R (2016) Toll-like receptor 4  
868 deficiency impairs motor coordination. *Front Neurosci* **10**,  
869 1-10.
- 870 [26] Brooks SP, Dunnett SB (2009) Tests to assess motor pheno-  
871 type in mice: A user's guide. *Nat Rev Neurosci* **10**, 519-529.
- 872 [27] Lopes S, Lopes A, Pinto V, Guimaraes MR, Sardinha VM,  
873 Duarte-Silva S, Pinheiro S, Pizarro J, Oliveira JF, Sousa N,  
874 Leite-Almeida H, Sotiropoulos I (2016) Absence of Tau trig-  
875 gers age-dependent sciatic nerve morphofunctional deficits  
876 and motor impairment. *Aging Cell* **15**, 208-216.
- 877 [28] Tricaud N, Perrin-Tricaud C, Brusés JL, Rutishauser U  
878 (2005) Adherens junctions in myelinating Schwann cells  
879 stabilize schmidt-lanterman incisures via recruitment of  
880 p120 catenin to E-cadherin. *J Neurosci* **25**, 3259-3269.
- 881 [29] Raj DD, Jaarsma D, Holtman IR, Olah M, Ferreira FM,  
882 Schaafsma W, Brouwer N, Meijer MM, de Waard MC,  
883 van der Pluijm I, Brandt R, Kreft KL, Laman JD, de  
884 Haan G, Biber KPH, Hoeijmakers JHJ, Eggen BJL, Bod-  
885 deke HWGM (2014) Priming of microglia in a DNA-repair  
886 deficient model of accelerated aging. *Neurobiol Aging* **35**,  
887 2147-2160.
- 888 [30] Spittaels K, Van den Haute C, Van Dorpe J, Bruynseels K,  
889 Vandezande K, Laenen I, Geerts H, Mercken M, Sciort R,  
890 Van Lommel A, Loos R, Van Leuven F (1999) Prominent  
891 axonopathy in the brain and spinal cord of transgenic mice  
892 overexpressing four-repeat human tau protein. *Am J Pathol*  
893 **155**, 2153-2165.
- 894 [31] Balkaya M, Kröber JM, Rex A, Endres M (2012) Assessing  
895 post-stroke behavior in mouse models of focal ischemia.  
896 *J Cereb Blood Flow Metab* **33**, 330-338.
- 897 [32] Stroobants S, Gantois I, Pooters T, D'Hooge R (2013)  
898 Increased gait variability in mice with small cerebellar cor-  
899 tex lesions and normal rotarod performance. *Behav Brain*  
900 *Res* **241**, 32-37.
- 901 [33] Roth L, Van Dam D, Van der Donckt C, Schrijvers DM,  
902 Lemmens K, Van Brussel I, De Deyn PP, Martinet W, De  
903 Meyer GRY (2015) Impaired gait pattern as a sensitive tool  
904 to assess hypoxic brain damage in a novel mouse model of  
905 atherosclerotic plaque rupture. *Physiol Behav* **139**, 397-402.
- 906 [34] Melis V, Zabke C, Stamer K, Magbagbeolu M, Schwab  
907 K, Marschall P, Veh RW, Bachmann S, Deiana S, Moreau  
908 PH, Davidson K, Harrington KA, Rickard JE, Horsley D,  
909 Garman R, Mazurkiewicz M, Niewiadomska G, Wischik  
910 CM, Harrington CR, Riedel G, Theuring F (2014) Different  
911 pathways of molecular pathophysiology underlie cognitive  
912 and motor tauopathy phenotypes in transgenic models for  
913 Alzheimer's disease and frontotemporal lobar degeneration. *Cell Mol Life Sci* **72**, 2199-2222.
- 914 [35] Ramsden M, Kotilinek L, Forster C, Paulson J, McGowan  
915 E, SantaCruz K, Guimaraes A, Yue M, Lewis J, Carlson G,  
916 Hutton M, Ashe KH (2005) Age-dependent neurofibrillary  
917 tangle formation, neuron loss, and memory impairment in a  
918 mouse model of human tauopathy (P301L). *J Neurosci* **25**,  
919 10637-10647.
- 920 [36] Schindowski K, Bretteville A, Leroy K, Bégard S, Brion  
921 J-P, Hamdane M, Buée L (2006) Alzheimer's disease-like  
922 tau neuropathology leads to memory deficits and loss of  
923 functional synapses in a novel mutated tau transgenic mouse  
924 without any motor deficits. *Am J Pathol* **169**, 599-616.
- 925 [37] Scattoni ML, Gasparini L, Alleva E, Goedert M, Calaman-  
926 drei G, Spillantini MG (2010) Early behavioural markers of  
927 disease in P301S tau transgenic mice. *Behav Brain Res* **208**,  
928 250-257.
- 929 [38] Allen B, Ingram E, Takao M, Smith MJ, Jakes R, Virdee  
930 K, Yoshida H, Holzer M, Craxton M, Emson PC, Atzori C,  
931 Migheli A, Crowther RA, Ghetti B, Spillantini MG, Goedert  
932 M (2002) Abundant tau filaments and nonapoptotic neuro-  
933 degeneration in transgenic mice expressing human P301S  
934 tau protein. *J Neurosci* **22**, 9340-9351.
- 935 [39] Terwel D, Lasrado R, Snauwaert J, Vandeweert E, Van  
936 Haesendonck C, Borghgraef P, Van Leuven F (2005)  
937 Changed conformation of mutant tau-P301L underlies  
938 the moribund tauopathy, absent in progressive, nonlethal  
939 axonopathy of tau-4R/2N transgenic mice. *J Biol Chem* **280**,  
940 3963-3973.
- 941 [40] Gonzalez-Freire M, de Cabo R, Studenski SA, Ferrucci L  
942 (2014) The neuromuscular junction: Aging at the cross-  
943 road between nerves and muscle. *Front Aging Neurosci* **6**,  
944 208.
- 945 [41] Pratt SJP, Shah SB, Ward CW, Inacio MP, Stains JP,  
946 Lovering RM (2013) Effects of in vivo injury on the neu-  
947 romuscular junction in healthy and dystrophic muscles.  
948 *J Physiol* **591**, 559-570.
- 949 [42] Ling KKY, Gibbs RM, Feng Z, Ko C-P (2012) Severe neu-  
950 romuscular denervation of clinically relevant muscles in a  
951 mouse model of spinal muscular atrophy. *Hum Mol Genet*  
952 **21**, 185-195.
- 953 [43] Moloney EB, de Winter F, Verhaagen J (2014) ALS as a  
954 distal axonopathy: Molecular mechanisms affecting neuro-  
955 muscular junction stability in the presymptomatic stages of  
956 the disease. *Front Neurosci* **8**, 252.
- 957 [44] Dadon-Nachum M, Melamed E, Offen D (2011) The  
958 "dying-back" phenomenon of motor neurons in ALS. *J Mol*  
959 *Neurosci* **43**, 470-477.
- 960 [45] Boido M, Vercelli A (2016) Neuromuscular junctions as  
961 key contributors and therapeutic targets in spinal muscular  
962 atrophy. *Front Neuroanat* **10**, 1-10.
- 963 [46] Zesiewicz TA, Baker MJ, Dunne PB, Hauser RA (2001)  
964 Diffuse Lewy body disease. *Curr Treat Options Neurol* **3**,  
965 507-518.
- 966 [47] Bennett GJ, Liu GK, Xiao WH, Jin HW, Siau C (2011)  
967 Terminal arbor degeneration—a novel lesion produced by  
968 the antineoplastic agent paclitaxel. *Eur J Neurosci* **33**, 1667-  
969 1676.
- 970 [48] Shi P, Gal J, Kwinter DM, Liu X, Zhu H (2010) Mitochon-  
971 drial dysfunction in amyotrophic lateral sclerosis. *Biochim*  
972 *Biophys Acta* **1802**, 45-51.
- 973 [49] Reddy PH (2011) Abnormal tau, mitochondrial dysfunction,  
974 impaired axonal transport of mitochondria, and synaptic  
975 deprivation in Alzheimer's disease. *Brain Res* **1415**, 136-  
976 148.
- 977

- 978 [50] Chang DTW, Honick AS, Reynolds IJ (2006) Mitochondrial  
979 trafficking to synapses in cultured primary cortical neurons.  
980 *J Neurosci* **26**, 7035-7045. 1021
- 981 [51] Dawson HN, Cantillana V, Jansen M, Wang H, Vitek MP,  
982 Wilcock DM, Lynch JR, Laskowitz DT (2010) Loss of tau  
983 elicits axonal degeneration in a mouse model of Alzheimer's  
984 disease. *Neuroscience* **169**, 516-531. 1022
- 985 [52] Smith KDB, Kallhoff V, Zheng H, Pautler RG (2007) In  
986 vivo axonal transport rates decrease in a mouse model of  
987 Alzheimer's disease. *Neuroimage* **35**, 1401-1408. 1023
- 988 [53] Sanchez-Varo R, Trujillo-Estrada L, Sanchez-Mejias E,  
989 Torres M, Baglietto-Vargas D, Moreno-Gonzalez I, De  
990 Castro V, Jimenez S, Ruano D, Vizquete M, Davila JC,  
991 Garcia-Verdugo JM, Jimenez AJ, Vitorica J, Gutierrez  
992 A (2012) Abnormal accumulation of autophagic vesicles  
993 correlates with axonal and synaptic pathology in young  
994 Alzheimer's mice hippocampus. *Acta Neuropathol* **123**,  
995 53-70. 1024
- 996 [54] Stamer K, Vogel R, Thies E, Mandelkow E, Mandelkow  
997 EM (2002) Tau blocks traffic of organelles, neurofilaments,  
998 and APP vesicles in neurons and enhances oxidative stress.  
999 *J Cell Biol* **156**, 1051-1063. 1025
- 1000 [55] Mandelkow EM, Stamer K, Vogel R, Thies E, Mandelkow E  
1001 (2003) Clogging of axons by tau, inhibition of axonal traffic  
1002 and starvation of synapses. *Neurobiol Aging* **24**, 1079-1085. 1026
- 1003 [56] Vossel KA, Zhang K, Brodbeck J, Daub AC, Sharma P,  
1004 Finkbeiner S, Cui B, Mucke L (2010) Tau reduction prevents  
1005 Abeta-induced defects in axonal transport. *Science* **330**, 198.  
1006 [57] Mizisin AP, Shelton GD, Wagner S, Rusbridge C, Pow-  
1007 ell HC (1998) myelin splitting, Schwann cell injury and  
1008 demyelination in feline diabetic neuropathy. *Acta Neu-  
1009 ropathol* **95**, 171-174. 1027
- 1010 [58] de Waegh S, Brady ST (1990) Altered slow axonal trans-  
1011 port and regeneration in a myelin-deficient mutant mouse:  
1012 The trembler as an in vivo model for Schwann cell-axon  
1013 interactions. *J Neurosci* **10**, 1855-1865. 1028
- 1014 [59] Schneider A, Araújo GW, Trajkovic K, Herrmann MM,  
1015 Merkler D, Mandelkow EM, Weissert R, Simons M (2004)  
1016 Hyperphosphorylation and aggregation of tau in experi-  
1017 mental autoimmune encephalomyelitis. *J Biol Chem* **279**,  
1018 55833-55839. 1029
- 1019 [60] Anderson JM, Hampton DW, Patani R, Pryce G, Crowther  
1020 RA, Reynolds R, Franklin RJM, Giovannoni G, Comp-  
1021 ston DAS, Baker D, Spillantini MG, Chandran S (2008)  
1022 Abnormally phosphorylated tau is associated with neu-  
1023 ronal and axonal loss in experimental autoimmune  
1024 encephalomyelitis and multiple sclerosis. *Brain* **131**, 1736-  
1025 1748. 1026
- [61] Kirkpatrick L, Brady T, Biology C, Southwestern T (1994)  
1027 Modulation of the axonal Schwann cells microtubule  
1028 cytoskeleton by myelinating. *J Neurosci* **14**, 7440-7450. 1027
- [62] Lisney SJ (1989) Regeneration of unmyelinated axons after  
1029 injury of mammalian peripheral nerve. *Q J Exp Physiol* **74**,  
1030 757-784. 1030
- [63] Jessen KR, Mirsky R (2016) The repair Schwann cell and its  
1031 function in regenerating nerves. *J Physiol* **594**, 3521-3531. 1032
- [64] Arthur-Farraj PJ, Latouche M, Wilton DK, Quintes S,  
1033 Chabrol E, Banerjee A, Woodhoo A, Jenkins B, Rahman M,  
1034 Turmaine M, Wicher GK, Mitter R, Greensmith L, Behrens  
1035 A, Raivich G, Mirsky R, Jessen KR (2012) c-Jun repro-  
1036 grams Schwann cells of injured nerves to generate a repair  
1037 cell essential for regeneration. *Neuron* **75**, 633-647. 1038
- [65] Vickland H, Silver J (1997) The role of astrocytes in  
1039 axon guidance during development and repair. In *Glial*  
1040 *Cell Development: Basic principles and clinical relevance*,  
1041 Jessen KR, Richardson WD, eds. Oxford, BIOS Scientific  
1042 Publishers, Herndon, VA, pp. 197-208. 1043
- [66] Sasaki A, Kawarabayashi T, Murakami T, Matsubara E,  
1044 Ikeda M, Hagiwara H, Westaway D, George-Hyslop PS,  
1045 Shoji M, Nakazato Y (2008) Microglial activation in brain  
1046 lesions with tau deposits: Comparison of human tauopathies  
1047 and tau transgenic mice TgTauP301L. *Brain Res* **1214**, 159-  
1048 168. 1048
- [67] Rotshenker S (2009) The role of Galectin-3/MAC-2 in the  
1049 activation of the innate-immune function of phagocytosis  
1050 in microglia in injury and disease. *J Mol Neurosci* **39**,  
1051 99-103. 1052
- [68] Nguyen JV, Soto I, Kim K-Y, Bushong EA, Oglesby E,  
1053 Valiente-Soriano FJ, Yang Z, Davis CO, Bedont JL, Son JL,  
1054 Wei JO, Buchman VL, Zack DJ, Vidal-Sanz M, Ellisman  
1055 MH, Marsh-Armstrong N (2011) Myelination transition  
1056 zone astrocytes are constitutively phagocytic and have synu-  
1057 clein dependent reactivity in glaucoma. *Proc Natl Acad Sci*  
1058 *U S A* **108**, 1176-1181. 1059
- [69] Reichert F, Saada A, Rotshenker S (1994) Peripheral nerve  
1060 injury induces Schwann cells to express two macrophage  
1061 phenotypes: Phagocytosis and the galactose-specific lectin  
1062 MAC-2. *J Neurosci* **14**, 3231-3245. 1063
- 1064